INTERNATIONAL JOURNAL FOR NUMERICAL AND ANALYTICAL METHODS IN GEOMECHANICS, VOL. 20, 431–442 (1996)

NUMERICAL STUDIES OF THE MOMENT CARRYING CAPACITY OF A SHORT PIER FOUNDATION IN A CLAY SOIL

G. J. W. KING

Department of Civil Engineering, University of Liverpool, Brownlon St. Liverpool, L69 3BX, U.K.

AND

M. LAMAN

Department of Civil Engineering, University of Cukurova, Turkey

SUMMARY

Numerical predictions of the immediate moment carrying capacity of a short pier foundation in saturated clay are presented. Three-dimensional finite element analyses are carried out using linear and non-linear programs and using a linear axi-symmetric program.

Preliminary investigations are made to determine suitable boundary distances for analysis at full-scale and size of loading increment for non-linear analyses.

Predictions of the behaviour of prototype pier and of conventional and centrifuge models of this pier are then made. It is shown that the axi-symmetric program yields significantly higher rotations per unit moment than the linear three-dimensional program and that, using both of these programs, elastic analyses of the conventional and centrifuge models and of the prototype yield very similar results. It is also shown that non-linear analyses of the conventional and centrifuge models yield significantly different moment/rotation relationship in accordance with the behaviour actually observed in the model tests. The relationship obtained for the centrifuge model is shown to differ only slightly from that obtained for the prototype, due to the boundary restrictions in the model, and to be of the same order as the centrifuge test result at working condition but not at ultimate capacity.

KEY WORDS: foundations; rigid pier; moment carrying capacity

1. INTRODUCTION

Foundations for transmission towers and gantries and for large road and railway hoardings and other elevated commercial signs have to be designed mainly to resist large moments and relatively small vertical and horizontal forces. A widely used type of foundation for these structures is the rigid pier.

In the past, the design of laterally loaded rigid pile and pier foundations has been based upon empirical information mainly from full-scale tests or conventional model studies in the laboratory. In recent years improved techniques have been developed for predicting the behaviour of these foundations which include centrifuge modelling and the finite element and boundary element methods.

In soil mechanics and foundation engineering one of the most rigorous numerical methods of solution is the finite element method. The method can permit realistic three-dimensional effects and computation of stresses and deformations in and around the piles. It is also possible to study progressive development of stresses and deformation leading to demarcation of failure zones.

CCC 0363–9061/96/060431–12
© 1996 by John Wiley & Sons, Ltd

Received 21 April 1995
Revised 15 November 1995

The method requires the use of a large computer for the solution of a given problem. Although the use of three-dimensional finite element analysis is relatively expensive, with the introduction of the new generation of computers and development of efficient solving and data storage routines, its use is becoming more common.

A simplification which has been used for axi-symmetric structures under non-axisymmetric loads is to express the circumferential displacements as Fourier series so that the analysis becomes two-dimensional. This method was first developed by Wilson[1] and was used for studying the problem of circular piers subjected to lateral loading by Desai and Chandrasekaran.[2]

This approach was also used by Chandrasekaran and King[3] for analysing the behaviour of laterally loaded piles embedded in an elastic continuum. Their computer program was written to allow consideration of arbitrary inhomogeneity in the soil deposit and also variable flexural rigidity along the length of piles.

Although the application of the finite element method to pile foundations has been described by several investigators, e.g. References[4-8], there is little published data which may be used to establish a rationale for the actual values of soil properties (such as shear modulus and its variation) which should be input into these analyses. Further, because of non-linearity of the stress–strain behaviour of soils, pile response to lateral loading is also non-linear. Although finite element programs are generally formulated for linear behaviour, incremental and/or iterative techniques can be used to simulate non-linear behaviour.

In this study, finite element analyses were carried out on a short, square, rigid pier when the top of the pier was subjected to a large overturning moment and relatively small vertical and horizontal force. Initially an existing two-dimensional (axi-symmetric) linear computer program was used and then three-dimensional linear and non-linear computer programs were developed. The results are compared with the results of conventional and centrifuge model tests, reported by Laman[9] and King and Laman.[10]

2. COMPUTER PROGRAM FOR TWO-DIMENSIONAL (AXI-SYMMETRIC) LINEAR ANALYSIS (PIER2D)

The finite element method based on harmonic representation of displacements in the circumferential direction, can be used for analysing a cylindrical pier subjected to a lateral load in an homogeneous elastic continuum (Wilson,[1] Cook[11]). The computer program used here was originally developed by Desai and Chandrasekaran[2] and incorporates horizontal and vertical friction elements beneath the base and sides of the piles and the continuum as shown in Figure 1. An automatic mesh generation routine to generate the entire model geometry has been added so that only the number of soil and foundation elements and the dimensions of the mesh subdivision, in each co-ordinate direction, have to be specified.

Eight-noded rectangular isoparametric elements are used to represent the pier and the soil medium, and six-noded, zero width, isoparametric friction elements are used to represent the horizontal and vertical interfaces between the pier and the soil continuum. In this study the friction elements were given very stiff parameters to simulate a perfectly rough interface.

A lateral load P applied in the $\theta = 0$ direction to the top of a pier of radius R is considered as a distributed horizontal load $p = P/(2\pi R)$, around the circumference of the pier, which comprises components

$$p_r = p\cos\theta \tag{1a}$$

and

$$p_\theta = -p\sin\theta \tag{1b}$$

in the r and θ directions, respectively.

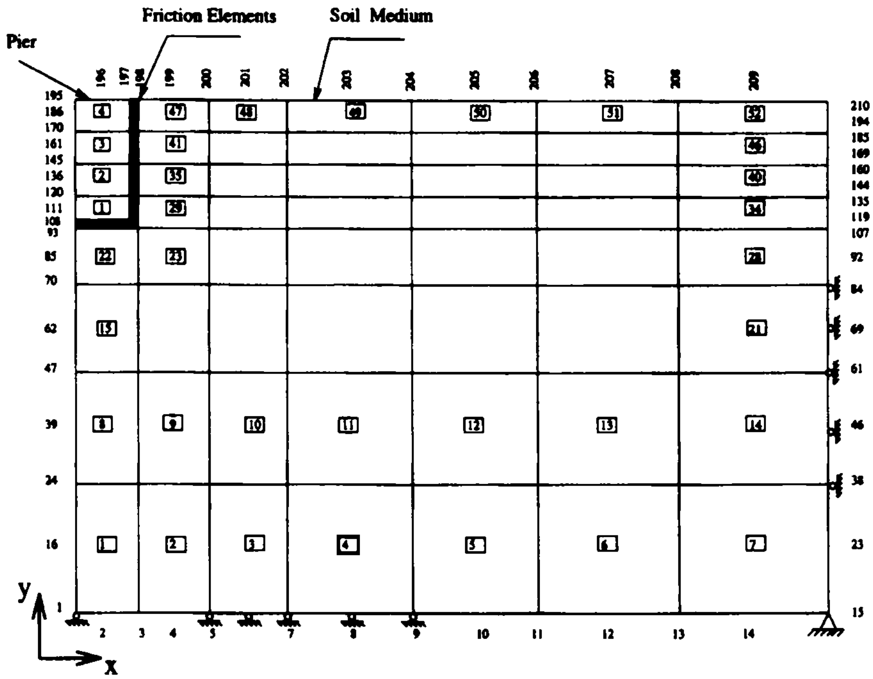

Figure 1. Finite element mesh for program PIER2D

A moment M applied in the $\theta = 0$ plane to the top of the pier is considered as a distributed vertical load

$$p_z = q \cos \theta \tag{2}$$

around the circumference of the pier such that

$$M = \int_0^{2\pi} R \cos \theta \, q \cos \theta \, R \, d\theta = \pi R^2 q \tag{3}$$

For equivalence of work done on the pier by the distributed loads moving through the circumferential displacements and by the equivalent nodal forces moving through the amplitudes of displacement, forces

$$P_r = \frac{P}{2}, \qquad P_\theta = -\frac{P}{2} \tag{4a}$$

and

$$P_z = \frac{M}{R} \tag{4b}$$

are applied at the node representing the top circumference of the pier. The listing of program PIER2D and the instructions for data preparation are given by Laman.[9]

3. COMPUTER PROGRAMS FOR THREE-DIMENSIONAL LINEAR AND NON-LINEAR ANALYSES (PIER3DLN AND PIER3DNL)

Although an axi-symmetric finite element analysis was first used to investigate the behaviour of a short pier foundation its application is of limited validity. It is well known that clays are not capable of holding tensile stresses. The tension behind the pier cannot be released simply by setting the normal stiffness of friction elements of zero because the axi-symmetric material properties associated with Fourier series cannot model this type of behaviour easily. Also only cylindrical piers can be analysed. Therefore three-dimensional finite element programmes were developed to perform both linear and non-linear analyses of rectilinear pier foundations.

Eight-node isoparametric brick elements were used for both soil and pier as shown in Figure 2. In both programs an automatic mesh generation routine was included which required only the number of nodes, number of soil and foundation elements and the co-ordinates of the nodal points along the x, y and z axes to be specified. The origin of the co-ordinate axes is node number 1. The numbering continues first in the z direction, then in the y direction and finally in the x direction. Elements are also numbered in the same order starting from the top element at the origin.

Force components are applied in the directions of the x, y and z axes. Moment components must be applied by means of equal and opposite vertical forces, distributed between the nodes along the front and rear top edges of the pier. In the linear program the soil can be specified as transversely isotropic or isotropic while the pier will usually be considered to be isotropic. It is possible to consider vertical inhomogeneity in the soil since the properties are given layer by layer.

In the linear analysis the soil and pier are assumed to be in contact at all times. However, since soil has limited ability to take tension, it is likely that separation occurs behind the pier at the top and in front of the pier at the bottom. In order to model this separation and the non-linearity of the soil's stress–strain behaviour, the isotropic hyperbolic stress–strain model used by Duncan and Chang[12] is incorporated into the non-linear program. A stress-dependent modulus for each element is calculated as

$$E_t = K\,p_a\left(\frac{\sigma_3}{p_a}\right)^n\left(1-\frac{R_f(\sigma_1-\sigma_3)\,(1-\sin\phi)}{2c\cos\phi+2\sigma_3\sin\phi}\right)^2 \tag{5}$$

for elements subjected to first time loading and as

$$E_{ur} = K_{ur}p_a\left(\frac{\sigma_3}{p_a}\right)^{n_{ur}} \tag{6}$$

for elements subjected to unloading, where K is the modulus number, p_a is atmospheric pressure, σ_1 and σ_3 are the major and minor principal stress, n is the modulus exponent, R_f is the failure ratio, c and ϕ are the apparent cohesion and apparent angle of internal friction of the soil and K_{ur} is the unloading–reloading modulus number.

The principal stresses are evaluated by solving the following equation (see Reference 13):

$$\sigma^3 - I_1\sigma^2 + I_2\sigma - I_3 = 0 \tag{7}$$

where

$$I_1 = \sigma_x + \sigma_y + \sigma_z$$

$$I_2 = \sigma_x\sigma_y + \sigma_y\sigma_z + \sigma_x\sigma_z - \tau_{xy}^2 - \tau_{yz}^2 - \tau_{zx}^2$$

and

$$I_3 = \sigma_x\sigma_y\sigma_z + 2\,\tau_{xy}\tau_{yz}\tau_{zx} - \sigma_x\tau_{yz}^2 - \sigma_y\tau_{xz}^2 - \sigma_z\,\tau_{xy}^2$$

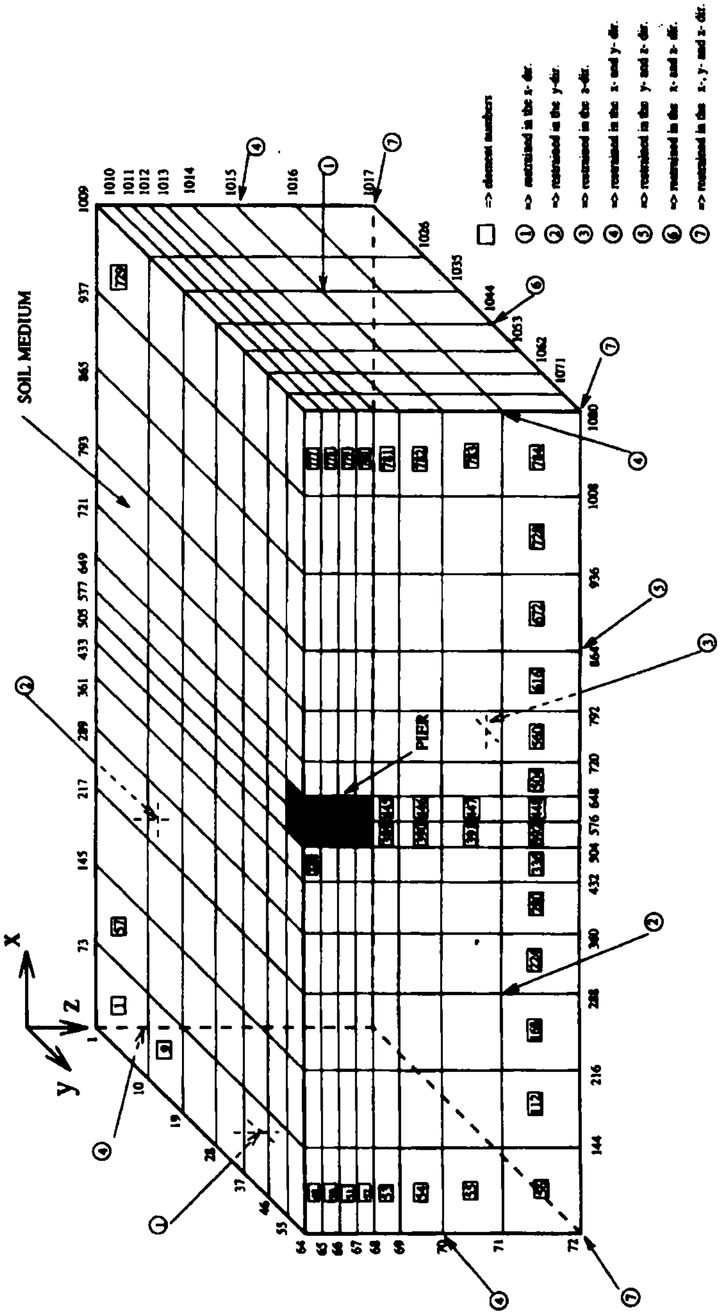

Figure 2. Finite element mesh for programs PIER3DLN and PIER3DNL

using the commercial mathematical package MATHEMATICA. The three roots are the principal stresses σ_1, σ_2 and σ_3.

The incremental analysis is performed as follows. The initial stresses due to self-wieght are calculated for all elements. The horizontal stresses, σ_x and σ_y, in an element are assumed to be equal to $K_0\,\sigma_z$, in which σ_z is the vertical stress in the element and K_0 is the coefficient of lateral earth pressure at rest. Shear stresses are set equal to zero for all elements. The load is then applied in increments and two iterations are performed for each increment. The modulus values for soil elements for the first iteration are based on the values of stress at the beginning of that increment. In the second iteration, refined values are based on the average values of stress at the beginning and end of the first iteration and on whether an element is being subjected to first time loading or unloading as defined by Dickin and King.[14] If tensile stresses are obtained in any soil element it is assigned a small value, $E_t = 1{\cdot}0$ kN/m^2. If an element fails in shear a small value, $E_t = 0{\cdot}5$ kN/m^2 is assigned.

At the end of each increment, the incremental nodal displacements and element stresses in soil and foundation elements are added to the previous total values to obtain the nodal displacements and element stresses at the end of the increment. The computer output can show the nodal displacements and element stresses at the end of each increment or only the final result as required.

Listings of programs PIER3DLN and PIER3DNL and instructions for data preparation are given by Laman.[9]

4. CONVENTIONAL AND CENTRIFUGE MODEL TESTS

The results of both conventional and centrifuge model studies of the moment carrying capacity of short square pier foundations in clay have been reported by King and Laman.[10] 1/40th scale model piers ranging from 20 to 60 mm square with embedment depths ranging from 20 to 60 mm were subjected to lateral loads applied at a constant height of 150 mm and with a constant rate of displacement of 0·4 mm/min. The variation of moment at ground level with rotation was observed up to a rotation of 5° which is well in excess of a permissible working rotation of 1 or 2°. The conventional tests were carried out in a bin 570 mm × 460 mm in plan using a depth of clay of 240 mm and the centrifuge tests in a bin 400 mm long × 460 mm wide filled to a depth of 180 mm. The general arrangement for both sets of tests were very similar and that for the centrifuge tests is illustrated in Figure 3.

The clay used was a remoulded silty clay which has a liquid limit of 42 per cent a plastic limit of 15 per cent and a range of moisture contents of 15–18 per cent and the clay beds were built up in layers approximately 40 mm thick using a standard compaction procedure. The degree of saturation in the clay was found to be between 97·5 and 100 per cent and from a series of undrained triaxial tests the variation of apparent cohesion with moisture content was found to be

$$\log_{10} c = 4{\cdot}4344 - 0{\cdot}1484m \tag{8}$$

where c is the cohesion in kN/m^2 and m the percentage moisture content. Consolidation tests on the clay in an oedometer showed that it has an equivalent pre-consolidation pressure of the order of 190 kN/m^2 and an average coefficient of consolidation of 0·465 m^2/yr.

Values of the hyperbolic parameters defined in equations (5) and (6), determined from undrained triaxial tests on the clay at a moisture content of 17 per cent are shown in Table I. Small

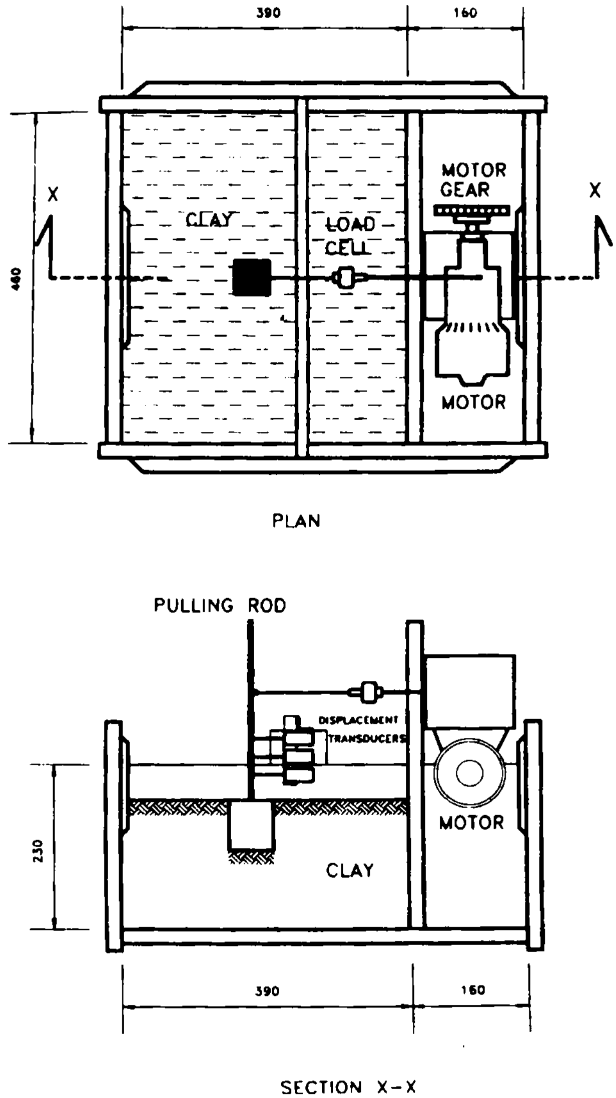

Figure 3. General arrangement of centrifuge test package (dimensions in mm)

differences in moisture content in different tests affected the strength and stiffness of the clay, and it was found that consistent results were obtained when results were expressed in terms of the ratio moment/cohesion.

A significant difference was observed between the behaviour in conventional and centrifuge tests and this is shown typically for tests on a 1·6 m square by 2·4 m depth prototype (40 mm square by 60 mm deep models) in Figure 4. Since the values of moisture content observed in the conventional and centrifuge tests were 16·43 and 17·29 per cent, respectively, the measured moment values have been corrected to a common moisture content of 17 per cent using ratios of the values of cohesion obtained from equation (8).

Table I. Soil parameters for non-linear analyses

Parameters	Values
Moisture content m	17·0%
Angle of internal friction ϕ	0·0°
Stiffnes exponents n, n_{ur}	0·0
Atmospheric presure, p_a	101·3 kN/m^2
Stiffness number, primary loading, K	16·47
Stiffness number, unloading–reloading K_{ur}	52·83
Cohesion, c	81.65 kN/m^2
Failure ratio, R_f	0·83
Bulk density, ρ	2148 kg/m^3
Poisson's ratio, ν_s	0·48
Coefficient of earth pressure at rest, K_0	1

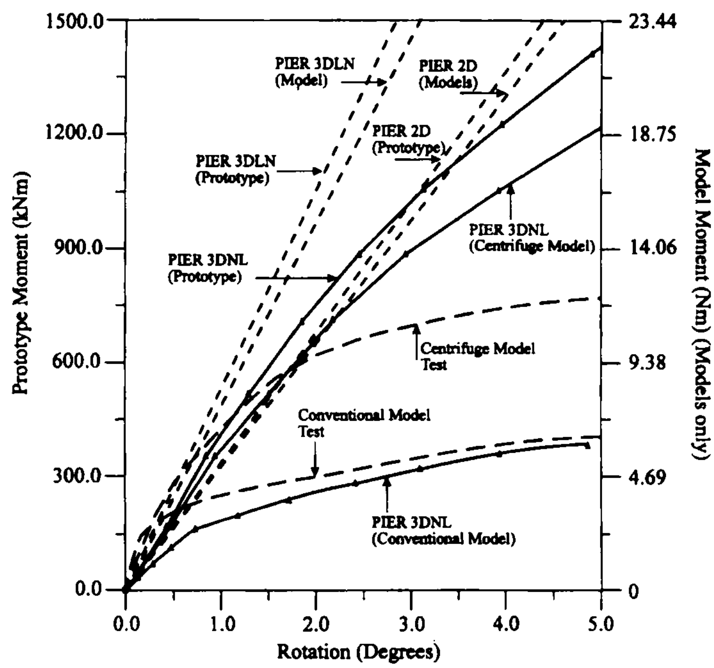

Figure 4. Comparison of experimental and computed moment-rotation curves

5. NUMERICAL STUDIES

The purpose of the numerical studies was to investigate the difference in the centrifuge and conventional model test results, to examine the influence of the artificial boundaries in the model studies and to consider the validity of the axis-symmetric formulation.

5.1. Axi-symmetric linear analysis using program PIER2D

The finite element mesh used is shown in Figure 1. The square pier with breadth B = 1·6 m and depth D = 2·4 m was subjected to a lateral load and moment applied at ground level to represent

Table II. Calculated rotations for different boundary distances (PIER2D)

Soil boundaries	$2{\cdot}5B =$ 2·22DIA = 4 m	$5B =$ 4·44DIA = 8 m	$7{\cdot}5B =$ 6·67DIA = 12 m	$10B =$ 8·89DIA = 16 m	$13B =$ 11·6DIA = 20.8 m	$20B =$ 18DIA = 32 m
Rottion	1·42°	1·38°	1·34°	1·33°	1·31°	1·308°

a lateral load applied at a height of 6 m. (This corresponds approximately to the height of overhead power lines supported by gantries for railways electrification. The nodes along the right-hand boundary were restrained in the horizontal direction, while the nodes at the bottom were restrained in the vertical direction, thus simulating smooth surfaces.

Since this program can only be used for analysing cylindrical piers, a suitable equivalent diameter had to be assumed. Taking equal areas this diameter, DIA $= 2B/\sqrt{\pi}$. Thus, the equivalent diameter of the 1·6 m breadth pier is 1·8 m.

The soil was assumed to be homogeneous and isotropic. Young's modulus was taken as 1668 kN/m^2 which is the initial tangent modulus of the clay at a moisture content of 17 per cent given by equation (5) and the parameters in Table I. Poisson's ratio for deformation without drainage is 0·5 and, since this value cannot be used directly in finite element analyses, a value of 0·48 was used. Young's modulus and Poisson's ratio for the pier were taken as 207×10^6 kN/m^2 and 0·25, respectively.

The pier was analysed under a nominal lateral load of 73·33 kN and the corresponding moment of 440·0 kNm applied at its top, since these values caused 1° rotation in the centrifuge test. The influence of the end boundary of the soil stratum was investigated by scaling the widths of the elements from the pier face to the boundary. The calculated rotations for a range of boundary distances and with a depth of stratum of $5B = 8$ m are shown in Table II. It is perhaps surprising that the calculated rotations decrease with increase in boundary distance. The lateral displacements at the top of the pier do increase but so does the depth to the point of rotation. Increasing the depth of the stratum also by scaling, showed no significant change in calculated rotations. Thus using this program, the influence of the end boundary appears to be significant until the boundary distance is at least $13B$.

Clearly the model boundaries will have some influence. Therefore in order to compare numerical results with the experimental results, analyses of the models were carried out using lateral boundary distances and stratum depths of $7{\cdot}1B$ and $6B$, respectively as in the conventional tests and $5B$ and $4{\cdot}5B$, respectively as in the centrifuge tests. Model load and moment values of $73{\cdot}33/40^2 = 0{\cdot}045833$ kN and $440{\cdot}0/40^3 = 0{\cdot}006875$ kNm, respectively, were applied at the top of the 40 mm square by 60 mm deep pier. The measured bulk density of the clay was used in the analysis of the conventional test while 40 time this value was used in the analysis of the centrifuge test in order to match the initial stress levels in that test. The calculated rotations were 1·36° in both analyses.

The corresponding linear relationships between moment and rotation are shown in Figure 4.

5.2. Three dimensional linear analysis using program PIER3DLN

Taking account of symmetry, the finite element mesh used is shown in Figure 2. The nodes on the end x–z and y–z planes were restrained in the y and x directions, respectively, whilst those on the bottom plane were restrained in the z direction. The same material properties and loadings were used as for the axi-symmetric analyses. The side boundaries were located at a distance of

Table III. Calculated rotations for different boundary distances (PIER3DLN)

Distance	$2{\cdot}5B = 4$ m	$4B = 6{\cdot}4$ m	$5B = 8$ m	$7{\cdot}5B = 12$ m	$10B = 16$ m	$20B = 32$ m
Rotation	1·10°	0·94°	0·93°	0·85°	0·83°	0·84°

Table IV. Calculated final rotations for different numbers of increments

Number of increments	1	2	5	10	20
Final rotation	10·91°	14·64°	18·20°	18·30°	18·29°

$5{\cdot}75B$ as used in both model studies and it was assumed that the influence of these boundaries would be negligible.

The influence of the end boundaries was investigated using the same material properties and loadings as specified in Section 5·1 and the calculated rotations for a range of boundary distances are shown in Table III for a depth of stratum of $5B = 8$ m. Increasing the depth of stratum showed no significant change in calculated rotations. Thus using this program, the influence of the end boundaries appears to be significant until the boundary distance is at least $7{\cdot}5B$.

Again for direct comparison of numerical results and experimental results analyses of the models were carried out using the restricted model boundary distances. The calculated rotations were almost identical, being 0·926° for the conventional test and 0·932° for the centrifuge test.

The corresponding linear relationships between moment and rotation are also included in Figure 4.

5.3. Three-dimensional non-linear analysis using program PIER3DNL

These were also carried out using the finite element mesh and boundary conditions specified in Section 5·2.

The material properties and the stress-dependent hyperbolic parameters given in Table I were used for the clay and Young's modulus and Poisson's ratio for the pier were again taken as 207×10^6 kN/m^2 and 0·25, respectively.

Preliminary calculations were made, using a large load of 500 kN and corresponding moment of 3000 kNm, to establish the influence of number of load increments used over a markedly non-linear range. The calculated rotations for a range of numbers of increments are given in Table IV. Since these showed little change after 10 increments it was decided that 10 increments would be more than adequate for studies involving smaller ranges of movement.

Analyses were then carried out to estimate behaviour at full scale using the artificial lateral boundary at a distance of $7{\cdot}5B$ and to predict behaviour in the model tests. Since the model tests were continued until the pier rotation reached about 5°, the load to be applied in each case was determined by trial and error using the results of the model studies as a guide. The moment rotation curves obtained are presented in Figure 4.

6. COMPARISON OF MOMENT/ROTATION RELATIONSHIPS FROM NUMERICAL AND EXPERIMENTAL RESULTS

6.1. Numerical predictions using the linear programs

The moment/rotation relationships predicted by the axi-symmetric and three-dimensional linear programs can be compared with each other, and with the behaviour observed in the model tests, in Figure 4.

Obviously neither of the programs gives results which match the test results, even at small rotations, nor do they predict that there should be any difference between behaviour in conventional and centrifuge model tests. The small differences between calculated predictions using the model geometries and prototype geometry can be attributed to the boundary restrictions in the models.

It is surprising that the axi-symmetric program predicts significantly more rotation per unit moment than the three-dimensional one, the difference being of the order of 50 per cent for prototype analyses.

6.2. Numerical predictions using the non-linear program

The moment/rotation relationships predicted by the three-dimensional non-linear program can be compared with the behaviour observed in the model studies in Figure 4. The numerical results clearly predict that there should be a difference in behaviour in conventional and centrifuge model tests. The results from the conventional model test and the corresponding finite-element analysis show good agreement at the higher rotations although the observed behaviour is initially stiffer. The corresponding results for the centrifuge model are in good agreement for pier rotations in the range of 0–2·5° but the agreement is not so good for larger rotations where the numerical prediction is appreciably stiffer than that observed. However, since working limits for pier rotation will invariably be less than 2·5°, the disagreement between numerical and experimental results for larger rotations is not of practical importance.

The significant difference in the behaviour in conventional and centrifuge model tests can be explained by considering the numerical analyses. Both models were analysed using model dimensions and loadings. However, the initial stresses in the conventional and centrifuge tests were calculated using unit weights for the clay of ρg and $40\rho g$, respectively. Thus after the application of only small increments of load, the stresses in elements behind the top and in front of the toe of the conventional model pier became tensile. These elements were then failed, by assigning them a negligible value of Young's modulus, and provided no resistance to further increments of load. Corresponding elements in the centrifuge model did not become tensile until after the application of at least four load increments.

The results of the numerical analyses of the centrifuge model and of the prototype are in good agreement, the small difference between them being attributable to the boundary restrictions in the model.

7. CONCLUSIONS

1. When analysing a pier foundation of breadth B and depth $1{\cdot}5B$, using the axi-symmetric and three-dimensional linear programs, it was found that the influence of the artificial vertical boundaries was insignificant when they were situated at distances of at least $13B$ and $7{\cdot}5B$, respectively, from the centre of the pier. Even then, these programs yielded results which

differed appreciably, the axi-symmetric one giving 50 per cent more rotation per unit moment. This suggests that the assumption of harmonic variation of stresses and displacements in the axi-symmetric formulation may not be appropriate for the analysis of non-circular piers and this is the subject of further investigation.

2. Linear elastic analyses of conventional and centrifuge models showed identical results and only differed from analyses at full-scale because of the boundary restriction in the models.
3. In incremental analyses, using the three-dimensional non-linear finite element program, it was found that 10 local increments were sufficient to give consistent results.
4. Non-linear three-dimensional analyses of conventional and centrifuge models showed significant difference in accord with behaviour observed in the tests. This was due to the earlier onset of tensile failure at the lower initial stress levels in the conventional tests. Thus even though conventional modelling is usually legitimate for studying the immediate bearing capacity of foundations in saturated clay, their rotational stability is significantly affected by self-weight stresses.
5. Non-linear three-dimensional analysis of the centrifuge model and of the prototype showed only small differences attributable to the boundary restrictions in the model.
6. When compared with the behaviour observed in the centrifuge model test, three-dimensional non-linear analysis, using hyperbolic soil parameters, under-predicts moments carrying capacity at small rotations but over-predicts at large rotations. Perhaps fortuitously, moment carrying capacities at acceptable working rotations of 1 or 2° are in good agreement.

REFERENCES

1. E. L. Wilson, 'Structural analysis of axisymmetric solids', *AIAA* (*U.S.A.*), **3**, 2269–2274 (1965).
2. L. D. Desai and V. S. Chandrasekaran, 'Displacements of laterally loaded circular wells', *Conf. Geotechnical Engineering*, Geotech 80, Bombay, (1980), pp. 165–170.
3. V. S. Chandrasekaran and G. J. W. King, 'Laterally loaded piles: finite element analysis and design and pilot centrifuge model studies', *Internal Report*, The University of Liverpool, 1982.
4. C. S. Desai and T. Kuppusamy, 'Application of a numerical procedure for laterally loaded structures', *Numer Methods Offshore Piling*, ICE, 93–99 (1980).
5. A. Verruijt and A. P. Kooijman, 'Laterally loaded piles in a layered elastic medium', *Geotechnique*, **39**, 39–46 (1989).
6. A. R. Selby and M. R. Arta, 'Three-Dimensional finite element analysis of pile groups under lateral loading', *Comput. Struct.* (*U.K.*), **40**, 1329–1336 (1991).
7. A. M. Trochanis, J. Bielak and P. Christiano, 'Three-dimensional nonlinear study of piles', *J. Geotechn. Eng. ASCE*, **117**, 429–47 (1991a).
8. A. M. Trochanis, J. Bielak and P. Christiano, 'Simplified model for analysis of one or two piles', *J. Geotechn. Eng. ASCE*, **117**, 448–466 (1991b).
9. M. Laman, 'The moment carrying capacity of short pier foundations in clay', *Ph.D. Thesis*, University of Liverpools, 1995.
10. G. J. W. King and M. Laman, 'Conventional and centrifuge model studies of the moment carrying capacity of short pier foundations in clay', *Can. Geotechn. J.* (1995), to be published.
11. R. D. Cook, *Concepts and Applications of Finite Element Analysis*, Wiley, New York, 1974.
12. J. M. Duncan and C. Y. Chang, 'Nonlinear analysis of stress and strain in soils', *J. Soil Mech. Found. Div. ASCE*, **96**, 1629–1653 (1970).
13. A. P. Boresi, O. M. Sidebottom, F. B. Seely and J. O. Smith, *Advanced Mechanics of Materials*, Wiley, New York, 1978.
14. E. A. Dickin and G. J. W. King, 'The behaviour of hyperbolic stress–strain models in triaxial and plane strain compression', *Int. Symp. on Numerical Models in Geomechanics*, Zurich, 1982, pp. 303–311.